Pergamon

Polyhedron Vol. 16, No. 23, pp. 4005–4015, 1997

0277–5387/97 \$17.00+0.00

PII: S0277–5387(97)00180–0

Heterocyclic systems containing tin(IV)—XIII [1]. Possible ceasing or inversion of the structural *trans* influence during the course of a bimolecular nucleophilic attack of a donor group in a series of Sn^{IV} rings

Mike Beuter, Ute Kolb, Andrea Zickgraf, Elmar Bräu, Michael Bletz and
Martin Dräger*

Institut für Anorganische Chemie und Analytische Chemie der Johannes Gutenberg-Universität,
D-55099 Mainz, Germany

(Received 19 March 1997; accepted 5 May 1997)

Abstract—In the series of the heterocycles $X[(CH_2)_3]_2SnR_2$ (16 newly synthesized compounds and two taken from the literature) and in the germanium analog $Bu^tN[(CH_2)_3]_2GeCl_2$, the donor group X (= NMe, NBz, NBu^t, NPr^i, O, S) intramolecularly attacks the Lewis acidic atoms Sn or Ge. Eight structure determinations (and, in addition, 2 taken from the literature) are compared. The nucleophilic attack at Sn is stronger for the ligands $R_2 = Cl_2$ than for the more electronegative $R_2 = (OSiPh_3)_2$. Overall the familiar *trans* influence holds: simultaneous approach of X and weakening of the ligand R(*trans*). In three cases of subtly graded donor strength a slight inversion or ceasing is observed: shorter distances $X \cdots Sn$ and simultaneously shorter distances Sn—R(*trans*). Also in a series of 8 compounds with $O \cdots Si$–(Hal) interaction, taken from the literature, the dominant *trans* influence ceases to zero in the central part of the oxygen approach. Actually, the discussed ranges of inversion or ceasing of the *trans* influence are small and in terms of e.s.d.s at the borderline of statistical significance. Despite this objection, the existence of four alike cases is noticeable. As an explanation for this secondary effect, a bonding scheme is discussed in which the electronegativity of the ligands inhibits the nucleophilic attack and in which its drive originates from the π-basicity of the ligands into a σ^*-LUMO at Sn or Ge. This bonding scheme is supported by semi-empirical MO calculations on the extended Hückel level for the Ge compound and its tetrahedral analogue $Cl_2GeBu^t_2$. In addition, a qualitative discussion of ^{119}Sn NMR chemical shifts is given, which uses the same line of arguments as applied above on the basis of interactions of frontier orbitals. © 1997 Elsevier Science Ltd

Keywords: tin; germanium; bimolecular nucleophilic attack; structural *trans* influence; frontier orbitals.

It is generally taken for granted that the attack of a donor atom at a Lewis acidic center simultaneously weakens the ligand in trans position. This structural *trans* influence is one of the basic facts from which Bürgi and Dunitz created their method of structure correlation [2]. By means of this method, it is possible to conclude chemical reaction pathways from crystal structure data. This approach was used to obtain a view of various reactions and it was especially extensively applied to follow the course of the bimolecular nucleophilic substitution (S_N2) [2]. The latter reaction is one of the most frequently investigated basic reactions in organic chemistry. Nevertheless, many details concerning this reaction are still uncertain [3].

With regard to the question of which properties of a molecule control a S_N2 reaction, we have recently synthesized the 27 heterocycles **1** (Scheme 1) [4]. Crys-

---

* Author to whom correspondence should be addressed.

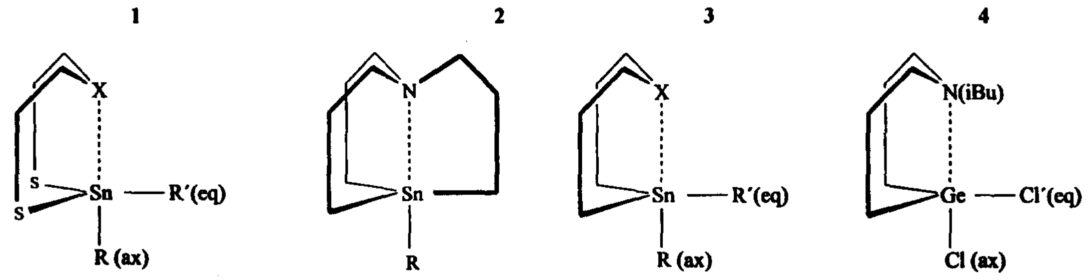

X	R / R'
NMe	Cl_2 Br_2 I_2 Me_2 Cl / Me Br / Me I / Me
O	
S	

R = F, Cl, Br, I

X	R / R'				
NMe	Cl_2	$(OSiPh_3)_2$	Cl / Ph	Ph_2	
NBz	Cl_2	$(OSiPh_3)_2$	Cl / Ph	Ph_2	
N(iBu)	Cl_2	$(OSiPh_3)_2$	Cl / Ph	Ph_2	
N(iPr)	Cl_2				
O	Cl_2	$(OSiPh_3)_2$		Ph_2	Br_2
S	Cl_2				

Scheme 1.

tal structure analyses, vibrations at the tin atom and ^{119}Sn NMR data outlined a step by step nucleophilic attack of X at the tin center [4]. To explain the results, the model of a four-electron, three-center interaction X$\cdots$Sn–R(*ax*) was created [4a], which originated in principle from a paper of Musher [5]. The σ-donor X attacks at the σ^*-LUMO of the acceptor Sn. A continuous transition from a tetrahedral into a trigonal-bipyramidal geometry occurs, and, simultaneously, a change of the hybridization takes place [4a,6]. The new LUMO of the pentacoordinate geometry [6] is located at lower energy than the LUMO of the starting geometry [4b,7]. The control of this path is affected by an interaction of the frontier orbitals at the acceptor, in which both kinds of ligands, axial and equatorial, are involved. The results lead to the unexpected thesis that an enhanced electronegativity of the ligands inhibits the formation of a pentacoordinate structure. The drive for pentacoordination results from the π-basicity of the ligands.

The series of compounds **2** shows especially clearly the mutual interaction of the polarity of the HOMO and of the occupation of the LUMO [8]: d(N$\cdots$Sn) = 2.38 Å for R = Cl and I; = 2.28 Å for R = Br. With regard to the sequence of strength of the donor atoms O and S [4], and with regard to the negative ligand F [9], the results were contradictory. For clarification, we synthesized and investigated 17 of the 18 compounds **3** and the Ge analog **4**. These compounds contain donors X of graded strength and the bulky ligand R = $OSiPh_3$, whose electronegativity is higher than that of R = Cl and for which no increase of coordination is to be expected.

RESULTS

Syntheses

To obtain the Cl_2 or ClPh substituted heterocycles **3** or **4**, the diGrignard reagent $X[(CH_2)_3MgCl]_2$ was reacted with $SnCl_4$, $PhSnCl_3$ or $GeCl_4$. The first examples of this diGrignard reaction, to obtain the compounds **3** (NMe/Cl_2, O/Cl_2 and S/Cl_2), had been carried out by Jurkschat [11]. The heterocycles with $(OSiPh_3)_2$ and Ph_2 substitution have been obtained from those with Cl_2 substitution by reaction with Ph_3SiONa or PhLi.

Molecular structures

Table 1 summarizes some distances at Sn and at Ge. Eight structure determinations have been carried out in this work; the data for the compounds **3** (NMe/Cl_2 and S/Cl_2) have been taken from ref. [11b]. The structure described for the compound **3** (O/Cl_2) in ref. [11b] is actually the structure of a mixed crystal with chlorine/bromine content [12]. The structural data of both pure compounds **3** (O/Cl_2 and O/Br_2) are given in Table 1.

The cores of all ten molecular structures discussed in this work look similar. Figure 1 shows exemplarily a plot of the compound **4** [N(Bu^i)/Cl_2], the plot of the compound **3** [N(Bu^i)/Cl_2] is nearly the same. In all ten structures, the geometry around tin or germanium and the twisting of the eight-membered rings [14] are very similar; i.e. distinct steric differences between the ten compounds do not exist. In addition, none of the

Table 1. Distances d and Pauling bond orders BO[a] for the heterocycles **3** and **4** (e.s.d.s in parentheses)

	Sn$\cdots$X		Sn—R(*ax*)		Sn—R′(*eq*)	
Compound	d (Å)	BO	d (Å)	BO	d (Å)	BO
3 (NMe/Cl$_2$)[b]	2.441(8)	0.320(8)	2.455(3)	0.735(8)	2.382(2)	0.94
3 (NMe/ClPh)	2.435(5)	0.326(5)	2.550(1)	0.540(2)	2.134(6)	1.05
3 (NBz/Cl$_2$)	2.470(5)	0.291(5)	2.487(2)	0.662(4)	2.420(1)	0.82
3 (NBz/(OSiPh$_3$)$_2$)	2.530(7)	0.240(6)	2.017(5)	0.95(1)	1.965(5)	1.12
3 (NBu^t/Cl$_2$)	2.462(3)	0.299(3)	2.474(1)	0.691(2)	2.379(1)	0.94
3 (NBu^t/(OSiPh$_3$)$_2$)	2.494(3)	0.269(3)	2.026(2)	0.92(1)	1.969(2)	1.11
3 (O/Cl$_2$)	2.448(8)	0.234(6)	2.465(2)	0.711(5)	2.410(3)	0.85
3 (O/Br$_2$)	2.421(7)	0.255(6)	2.574(1)	0.786(3)	2.509(1)	0.97
3 (S/Cl$_2$)[b]	2.851(3)	0.231(3)	2.449(3)	0.749(7)	2.375(3)	0.95
4 (NBu^t/Cl$_2$)[c]	2.389(4)[c]	0.180(2)	2.319(2)[c]	0.559(3)	2.186(2)[c]	0.86

[a] See ref. [15].

[b] Data taken from ref. [11b]; the compound **3**(S/Cl$_2$) has not been synthesized in this work.

[c] Ge$\cdots$N and Ge—Cl.

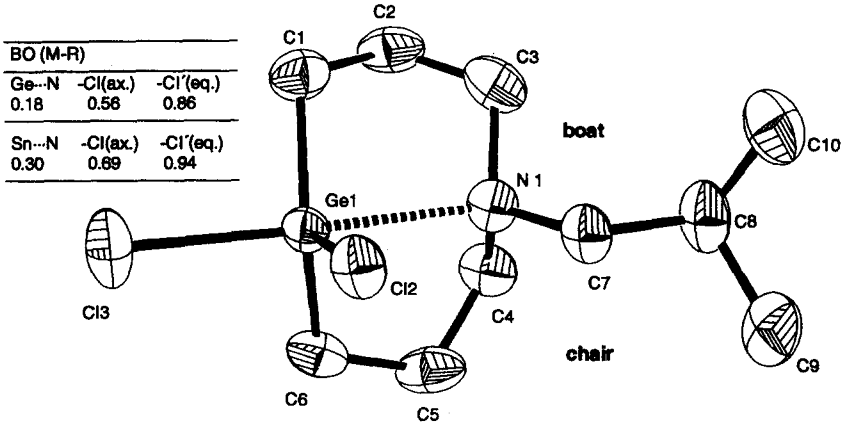

Fig. 1. Ortep plot of the compound **4**(NBu^t/Cl$_2$); thermal ellipsoids are at the 50% probability level. Hydrogen atoms are omitted for better clarity. The plot of the compound **3**(NBu^t/Cl$_2$) looks nearly the same. The Pauling bond orders BO [15] at Ge and Sn are compared: three-times long distances for the germanium compound, and three-times short distances for its tin analogue.

molecules of Table 1 is involved in short intermolecular interactions which would disturb the distances given in Table 1.

In order to obtain a comparability of the distances between atoms of different kinds, all distances *d* in Table 1 have been transformed into Pauling bond orders BO [15], which change inversely to *d*.

^{119}Sn *NMR data*

Table 2 contains the ^{119}Sn NMR chemical shifts and the one-bond spin–spin coupling constants between ^{119}Sn and the aliphatic ^{13}C of the methylene groups in equatorial position for all compounds of the series **3**. Both figures are indicative for a pentacoordinated tin atom [17]. In addition, Table 2 contains the equivalent figures of some related compounds with tetracoordinated tin and (methyl, *n*-butyl or phenyl)-substitution. The ^{29}Si NMR chemical shifts of the equatorial and axial OSiPh$_3$ groups are given in footnote *b* of Table 2. A full set of the ^{13}C NMR chemical shifts of the compounds **3** and **4** has been deposited with the Editor as supplementary material.

DISCUSSION

Electronegativity

By comparing the Sn$\cdots$X bond orders of Table 1, it is evident that the interaction between Sn and X generally increases with decreasing electronegativity of the ligands [19]. The polarity of the HOMOs and the occupation of the LUMO (*vide infra*) are counteractive [4a].

Table 2. ^{119}Sn NMR chemical shifts $\delta(^{119}Sn)$ and one-bond coupling constants $^1J(^{119}Sn—^{13}C)$ to the equatorial methylene groups of the compound series **3** (ambient temperature, $CDCl_3$ solution) and, for comparison, of some related compounds with 4-coordinated tin

Compound	δ (ppm)	^1J (Hz)
3 (NMe/Cl_2)[a]	−14.3	609.7
3 (NMe/$(OSiPh_3)_2$)[b]	−123.9	682.3
3 (NMe/ClPh)	−54.8	535.5
3 (NMe/Ph_2)	−103.4	459.0
3 (NBz/Cl_2)	−6.7	598.2
3 (NBz/$(OSiPh_3)_2$)[b]	−117.1	671.6
3 (NBz/ClPh)	−42.2	528.3
3 (NBz/Ph_2)	−94.6	448.6
3 (NBu^i/Cl_2)	−1.5	601.2
3 (NBu^i/$(OSiPh_3)_2$)[b]	−114.3	673.3
3 (NBu^i/ClPh)	−35.4	527.8
3 (NBu^i/Ph_2)	−91.4	447.8
3 (NPr^i/Cl_2)	−2.9	592.2
3 (O/Cl_2)[c]	+5.1	599.0
3 (O/Br_2)	−28.8	566.5
3 (O/$(OSiPh_3)_2$)[b]	−115.8	670.5
3 (O/Ph_2)	−86.0	430.2
3 (S/Cl_2)[d]	+19.8	561.0
Bu^n_4Sn[e]	−11.5	313.7
$Bu^n_2SnPh_2$[e]	−65.9	
$Bu^n_2SnCl_2$[f]	+122.0	424.0
Me_4Sn[e]	0.0	337.8[g]
Me_3SnPh[e]	−28.6	347.5[g]
Me_2SnPh_2[e]	−60.0	365.0[g]
$MeSnPh_3$[e]	−93.0	377.0[g]
$SnPh_4$[e]	−128.1	—

[a] This work; ref. [11b]: −14.8 and 612.4.

[b] $\delta(^{29}Si)$: $O(SiPh_3)_2$ −18.45; **3**NMe/$(OSiPh_3)_2$ −19.66 (*eq*) and −24.61 (*ax*); NBz/$(OSiPh_3)_2$ −19.51 (*eq*) and −24.29 (*ax*); N(iBu)/$(OSiPh_3)_2$ −19.42 (*eq*) and −24.59 (*ax*); O/$(OSiPh_3)_2$ −21.80 (one broad signal only).

[c] This work; ref. [11b]: −28.46 and 571.0, see ref. [12].

[d] Ref. [11b], toluene-d_8 solution; the compound has not been synthesized in this work.

[e] Ref. [17b].

[f] Ref. [18].

[g] One-bond coupling to methyl.

Structural trans *influence*

Figure 2 compares the bond orders BO(Sn···X) with the bond orders to the axial ligand R(*ax*). With regard to the sequence of the ligands $(OSiPh_3)_2$–Cl_2–ClPh and a general nitrogen donor NR, the normal *trans* influence of a σ-donor attack is valid. The bond to the axial ligand expands uniformly with an approach of the donor NR. The same holds for constant substitution Cl_2 if the donors O or S are changed into NR.

The normal *trans* influence inverts in the cases of constant Cl_2 substitution if a sequence of nitrogen donors NR is followed. Along the series of the compounds **4** (NBu^i/Cl_2)–**3** (NBz/Cl_2)–**3** (NBu^i/Cl_2)–**3** (NMe/Cl_2), the donor NR approaches the tin atom and simultaneously the distances between tin and the axial ligand Cl(*ax*) decrease. Actually, the inversion is small and in terms of e.s.d.s at the borderline of statistical significance: distance range merely 0.03 Å in *d*(Sn···N) (4 e.s.d.s) and *d*(Sn—Cl) (11 e.s.d.s), respectively. The inversion becomes only significant if the germanium case **4** is included (Fig. 1): ranges of bond order differences Ge/Sn about 0.12 (15 e.s.d.s in BO). The inversion is a secondary effect which overrides the dominant normal *trans* influence only slightly.

An equivalent inversion of the *trans* influence holds for the sequence of halide substituted compounds **3** (O/Cl_2)–**3** (O/Br_2) with BO(Sn···O) 0.23–0.25 and BO(Sn—Cl/Sn—Br) 0.71–0.79. For the sake of clarity, this relation is not indicated in Fig. 2. Also in this case, the inversion range is small: 0.03 Å in d(Sn···O) (3 e.s.d.s) and 0.08 in BO(Sn–halide) (15 e.s.d.s).

No difference of the donor strength exists between the atoms O and S in the case of constant Cl_2 substitution (Fig. 2); the counteractive effects, normal and inverted *trans* influence, cancel each other. This is the reason for the contradictory results, which were found for the sequence of the donor atoms O and S in the series of compounds **1** [4].

In a related series of eight β-lactams an O···Si approach influences Si–(halide) distances [20]. Overall the structural *trans* influence is active. However in the central part of this series, the change of the Si—Cl distances almost ceases. The given results for five O···Si—Cl pairs are [20]: 2.425/2.148, 1.990/2.309, 1.954/2.307, 1.950/2.315, 1.918/2.348 Å. Over a Si···O range of 0.04 Å the Si—Cl distance is almost constant.

In each of the mentioned four cases, the objection 'none full statistical significance' is valid. Nevertheless, the existence of four alike cases is noticeable. An inversion or ceasing of the overall *trans* influence can be caused by a charge flow from the ligand Cl(*ax*) into the LUMO of the molecule. The graded donor strength of the nitrogen donors or the change from germanium to the more acidic tin reveals the π-basic charge flow as a controlling factor of the nucleophilic attack at group 14 atoms.

Extended Hückel calculations

The question which of the two counteracting properties of a ligand, electronegativity or π-basicity, inhibits and which promotes a nucleophilic attack at Ge or Sn depends crucially upon the energetical position of the LUMO of the molecule: location in the bonding or in the antibonding region. In ref. [4b], the sequence of bond orders BO(Sn···X) for the axial and equatorial ligands halide and methyl in the series of compounds **1** offered evidence that the LUMO is located in the bonding region. To aid in making a direct decision, semi-empirical MO calculations on the extended Hückel level for the compound **4** and its

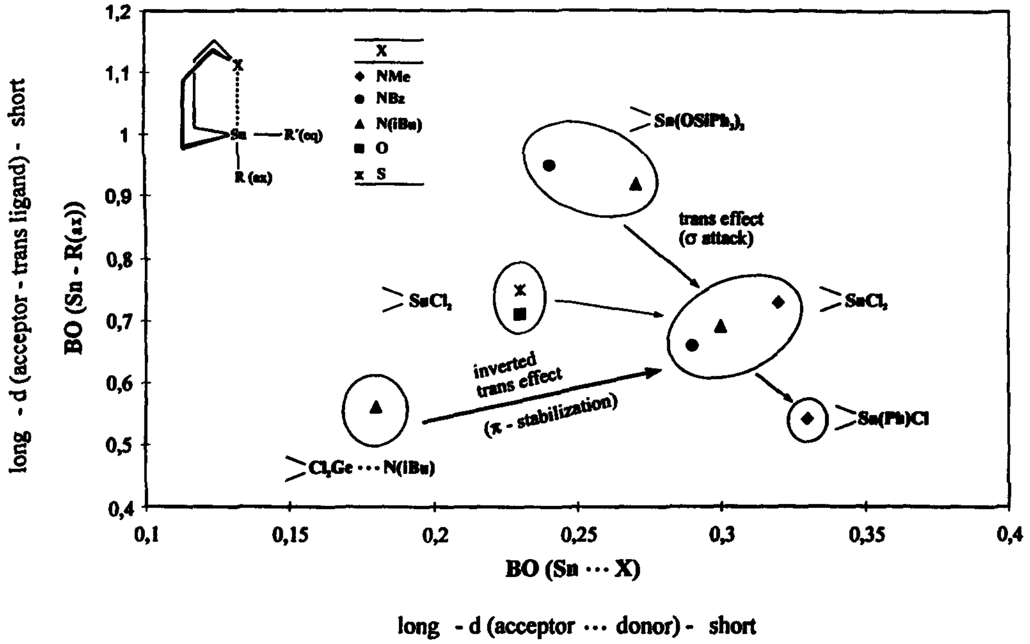

Fig. 2. Graph of the Pauling bond orders BO(Sn—R(*ax*)) *vs* BO(Sn···X) for the compounds **3** and **4**.

tetrahedral analogue $Cl_2GeBu^n_2$ were undertaken [21]. For **4** the geometry of the crystal structure determination has been fixed [21a], for $Cl_2GeBu^n_2$ a tetrahedral geometry has been chosen by means of the internal force field parameters of the program [21b]. The results are shown in Fig. 3 [22].

The extended Hückel approximation results only in a qualitative sequence of the MO's, and the absolute values of the energy scale of Fig. 3 should be considered with caution. Nevertheless, the overall view of Fig. 3 is in accord with the bonding scheme of ref. [4a]. The two HOMO's of the 4-electron, 3-center interaction and the σ^*-LUMO of the pentacoordinated geometry are distinctly separated from the sequence of the other occupied and empty MO's. In addition, the LUMO of the pentacoordinated

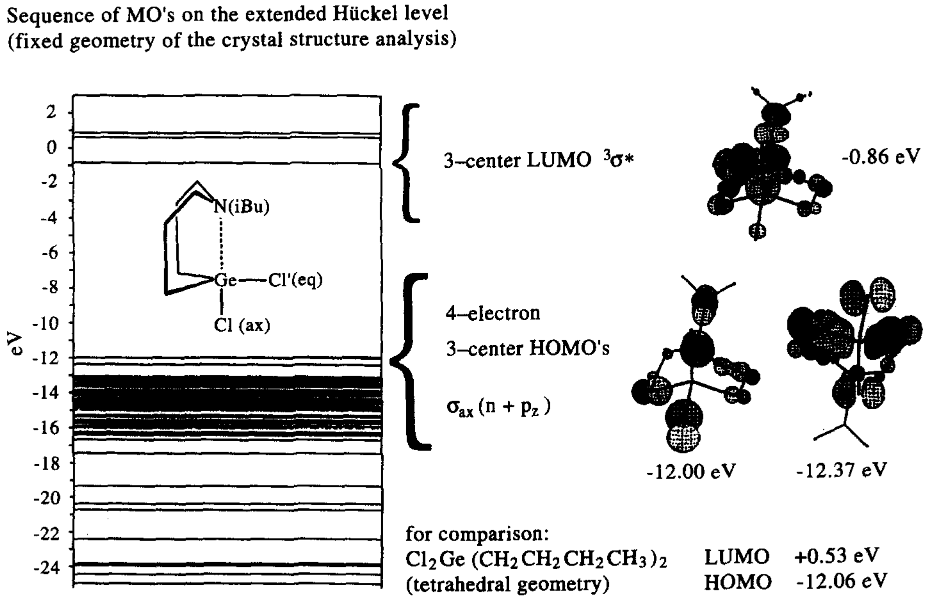

Fig. 3. Sequence of the MO's for the compound **4** in terms of CACAO-graphs [21a]. The LUMO and HOMO energies for the tetrahedral analogue $Cl_2GeBu^n_2$ are given for comparison [21b]. For the used nomenclature see ref. [6], for the extended Hückel parameters see ref. [22].

geometry is noticeably lower in comparison to the LUMO of the tetracoordinated geometry. With regard to the question, location of the LUMO of pentacoordination in the bonding region or not, the calculated value of -0.86 eV should not be interpreted too literally. The same reservation holds for a comparison of the numerical energy values of the HOMO's of the pentacoordinated state with those of the tetrahedral state.

^{119}Sn *NMR chemical shifts*

Generally, NMR parameters depend upon a rather subtle interplay of several factors [23]. Chemically and structurally strongly related systems must be chosen for any discussion of a specific factor. Such a condition is fulfilled in the series of compounds **3** of this work, and the factors which will be discussed in the following are on the one hand the polarity and the alignment of the HOMO's and on the other hand the occupation of the LUMO.

Figure 4 visualizes the spreading of the data of Table 2. According to the ligands at the tin atoms, four well-separated groups of signals are discernible. With regard to $\delta(^{119}Sn)$, the main influence arises from the number of phenyl groups at the tin atom; a roughly linear upfield shift upon an increase of this number exists. An equivalent linear upfield shift holds along the tetra-coordinated series $Me_{4-n}SnPh_n$ ($n = 0$–4) (Table 2). An increasing charge flow from the aromatic phenyl groups into the σ^*-LUMO results in a more and more shielded ^{119}Sn nucleus [24].

The deshielding electronegativity of ligands at tin acts opposite to the shielding by phenyl groups [25]. In contrast, the shielding pentacoordination acts in the same direction as a phenyl group. This effect is known for a long time [17a]. An explanation was given in ref. [4a] in terms of higher electron densities due to the 4-electron, 3-center interaction and due to the occupation of the σ^*-LUMO. For this explanation, an especially high population of the LUMO should be assumed for the compounds **3** with $(OSiPh_3)_2$ substitution, as the ^{119}Sn signals are at the highest field of all compounds in Fig. 4. The occupation of the LUMO cancels the strong electronegativity of oxygen, which on the one hand inhibits the pentacoordination and on the other hand gives rise to a downfield shift. In summary, it can be concluded from Fig. 4 that, irrespective of all other influences, the occupation of the LUMO is the predominant promoter of an upfield shift.

^{119}Sn *NMR spin–spin coupling*

For the equatorial one-bond coupling constants, the common discussion is based on the percentage of s-electron density at both involved nuclei in terms of different states of hybridization [17a]. An equivalent discussion in terms of the alignment of the HOMO's was given in ref. [8] for the severely strained compounds **2**. However, if the goodness of the trigonal bipyramids [26] in the series of the three compounds **3** (NMe/Cl_2)–**3** ($NMe/PhCl$)–**3** ($NBu^i/(SiOPh_3)_2$), 61–70–61°, is compared with the sequence of ^1J in Fig. 4, it is evident that such a one-dimensional argumentation is too much of a simplification, and that additional factors must be involved.

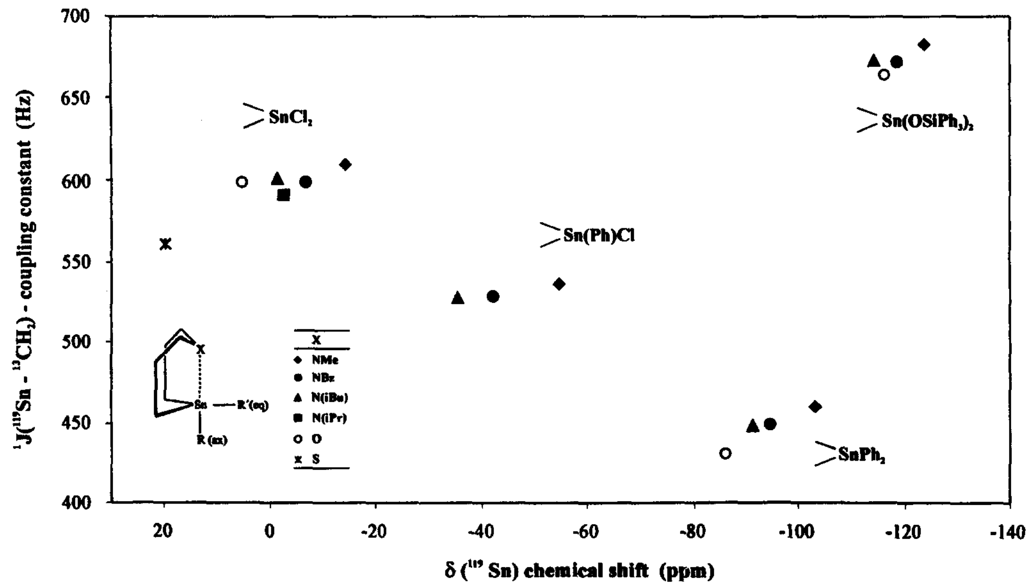

Fig. 4. Plot of the one-bond NMR-coupling constants between ^{119}Sn and ^{13}C (α-methylene) *vs* the ^{119}Sn chemical shifts for the heterocycles **3**.

EXPERIMENTAL

General procedures

The starting ligands $X[(CH_2)_3Cl]_2$ and $O[(CH_2)_3Br]_2$ and the related diGrignard reagents were prepared as described previously [13]. The use of the Grignard starter dibromo ethane must be avoided as otherwise the final product is inevitably contaminated with bromine [13]. The reagent Ph_3SiONa was obtained by reaction of Ph_3SiOH with sodium in toluene. Elemental analyses were carried out by the Microanalytical Laboratory of the Institut für Organische Chemie, Universität Mainz. EI mass spectra were taken on a Finnigan 8230 spectrometer. NMR spectra were recorded on a Bruker WP-80/DS FT-NMR spectrometer at 20.15 (^{13}C), 28.88 (^{119}Sn) and 15.92 (^{29}Si) MHz (solvent $CDCl_3$; ambient temperature; external standards $SiMe_4$ and $SnMe_4$).

Preparations of **3** *and* **4**

The diGrignard reaction must be carried out in a highly diluted solution. 0.05 mol of the diGrignard reagent in 125 ml THF and 0.05 mol $SnCl_4$ (or $SnBr_4$, $PhSnCl_3$, $GeCl_4$) in 125 ml toluene were added simultaneously and dropwise into 1 L toluene contained in a three-necked 2 L flask with vigorous stirring over a period of 1.5 h. The stirring was continued in the case of **3** with reflux for 2 h and in the case of **4** at room temperature for 24 h. The reaction mixtures were filtered several times, still hot in the case of **3**, to remove the formed $MgCl_2$ as completely as possible. The solvent was removed under vacuum, and the products were recrystallized from ethanol until no $MgCl_2$ was left. All compounds are solid and colourless. To obtain the compounds with $(OSiPh_3)_2$ substitution, a clear solution of 0.02 mol Ph_3SiONa in 100 ml toluene was added dropwise and under reflux into a vigorously stirred suspension of 0.01 mol **3**(X/Cl_2) in 100 ml toluene. A local excess of Ph_3SiONa must be avoided as otherwise $O(SiPh_3)_2$ forms. The refluxing was continued for 3 h and the mixture was filtered still hot. The solvent was removed under vacuum and the products were recrystallized from ethanol. All compounds are solid and colourless. To obtain the compounds with Ph_2 substitution, a solution of 0.02 mol PhLi in 15 ml *n*-hexane was added with stirring at −70°C into a suspension of 0.01 mol **3**(X/Cl_2) in 100 ml ether. The stirring was continued for 1 h, and subsequently the mixture was slowly warmed to room temperature. 30 ml H_2O was added. The organic phase was separated and dried over Na_2SO_4. The solvent was removed under vacuum and the residue was distilled *in vacuo*. The compounds are light yellow oils of high viscosity; only **3**(O/Ph_2) could be solidified. Table 3 summarizes the yields and the analytical data for the 18 synthesized compounds.

X-ray crystallography

Single crystals were obtained from ethanol [**3**$(NBz/Cl_2$, NBu^i/Cl_2, $NBz/(OSiPh_3)_2$, $NBu^i/(OSiPh_3)_2)$ and **4**], from $CHCl_3$ [**3**$(O/Cl_2$ and $O/Br_2)$] and from toluene [**3**(NMe/ClPh)]. A summary of the crystal data, of the intensity data collections and of the refinements is given in Table 4. The densities were determined by flotation in aqueous polytungstate solution. The quality and the symmetry of the crystals were examined by Weissenberg exposures. Integrated intensities were measured by means of $\omega/2\theta$ scans on an Enraf–Nonius CAD4 diffractometer. The structures were solved by Patterson syntheses (Sn, Hal, Ge; program SHELX-86) and completed by Fourier syntheses (C, N, O; SHELX-76). The refinements, partly on $|F|$ by program SHELX-76, partly on $|F|^2$ by program SHELX-93, resulted in good convergences and in even distributions of the variances. Hydrogen atoms were calculated and refined as riding on their carbon atoms. The compound **3**$(NBz/(OSiPh_3)_2)$ crystallizes in the noncentrosymmetric space group $P2_12_12_1$. The ratio of the weighted *R*s inverted/chosen structure is 1.057, which corresponds to a significance level on 99.9%. Details of crystal data and structure determinations, ORTEP views, tables of positional and thermal parameters, bond lengths, bond angles and torsion angles have been deposited with the Editor as supplementary material.

CONCLUSIONS

Both results, the experimental ones of the structure determinations and the calculations on the extended Hückel level, support the view that the π-basicity of the ligands at germanium or tin promotes the nucleophilic attack on these atoms, and that the electronegativity of the ligands inhibits this attack. However, the crystallographic effects are at the borderline of statistical significance, and more experimental evidence and an *ab initio* calculation are needed.

In view of the discussed bonding scheme, both atoms, Ge and Sn, own two different types of acidity: σ-acidity with regard to the donor and π-acidity with regard to the ligands. It can be considered that the sequence of both types of acidity must not necessarily change in a fully parallel manner in Group 14, and that at least some of the known irregular trends in chemical reactivity along the series Si–Ge–Sn–Pb can be attributed to such an effect.

Acknowledgements—We are grateful for financial assistance from the Deutsche Forschungsgemeinschaft, Bonn, Germany, and from the Fonds der Chemischen Industrie, Frankfurt/Main, Germany. We thank Klaus Jurkschat, Universität Dortmund, Germany, who personally introduced us to his work with the diGrignard reaction. We thank Carlo Mealli, C. N. R. Firenze, Italy, who provided an actual version of his program CACAO.

Table 3. Preparation and analytical data for **3** and **4**

				Anal. found (calcd)			
Compound	Method yield (%)	Formula M_r	M.p. (°C) m/e[a] (%)	%C	%H	%N	%Hal
3 (NMe/Cl$_2$)	diGrignard	$C_7H_{15}Cl_2NSn$	158	27.73	4.83	4.63	22.29
	60[b]	302.82	268[c] (16)	(27.76)	(4.99)	(4.63)	(23.42)
3 (NBz/Cl$_2$)	diGrignard	$C_{13}H_{19}Cl_2NSn$	212	41.15	4.99	3.69	17.53
	34	378.92	379 (1)	(41.21)	(5.05)	(3.70)	(18.71)
3 (NBu^i/Cl$_2$)	diGrignard	$C_{10}H_{21}Cl_2NSn$	154	34.53	6.10	3.90	19.15
	35	344.90	346 (9)	(34.82)	(6.14)	(4.06)	(20.56)
3 (NPr^i/Cl$_2$)	diGrignard	$C_9H_{19}Cl_2NSn$	112	31.55	5.60	4.12	21.38
	7	330.87	296[c] (22)	(32.67)	(5.79)	(4.23)	(21.43)
3 (O/Cl$_2$)	diGrignard	$C_6H_{12}Cl_2OSn$	150	23.58	4.17		22.97
	7	289.78	292 (2)	(24.87)	(4.17)		(24.47)
3 (NMe/(OSiPh$_3$)$_2$)	Ph$_3$SiONa	$C_{43}H_{45}NO_2Si_2Sn$	147	66.56	6.54	1.89	
	76	782.72	508[d]	(65.98)	(5.80)	(1.79)	
3 (NBz/(OSiPh$_3$)$_2$)	Ph$_3$SiONa	$C_{49}H_{49}NO_2Si_2Sn$	152	69.80	6.33	1.68	
	73	858.82	535[f]	(68.53)	(5.75)	(1.63)	
3 (NBu^i/(OSiPh$_3$)$_2$)	Ph$_3$SiONa	$C_{46}H_{51}NO_2Si_2Sn$	164	67.84	6.89	1.98	
	71	824.89	783[e]	(66.99)	(6.23)	(1.70)	
3 (O/(OSiPh$_3$)$_2$)	Ph$_3$SiONa	$C_{42}H_{42}O_3Si_2Sn$	114	65.56	5.37		
	70	769.68	694[h,i] (16)	(65.54)	(5.50)		
3 (NMe/ClPh)	diGrignard	$C_{13}H_{20}ClNSn$	179	43.38	5.85	3.77	10.35
	25	344.47	310[c] (21)	(45.33)	(5.85)	(4.07)	(10.29)
3 (NBz/ClPh)	diGrignard	$C_{19}H_{24}ClNSn$	190	52.80	5.03	3.35	9.37
	9	420.57	421 (1)	(54.26)	(5.75)	(3.33)	(8.43)
3 (NBu^i/ClPh)	diGrignard	$C_{16}H_{26}ClNSn$	123	47.52	6.58	3.81	10.31
	15	386.55	388 (1)	(49.72)	(6.78)	(3.62)	(9.17)
3 (NMe/Ph$_2$)	PhLi	$C_{19}H_{25}NSn$	198 (0.05)[g]	59.31	6.51	3.56	
	43	386.13	310[h] (100)	(59.10)	(6.53)	(3.63)	
3 (NBz/Ph$_2$)	PhLi	$C_{25}H_{29}NSn$	220 (0.05)[g]	64.96	6.70	3.09	
	63	462.22	387[h] (100)	(64.96)	(6.32)	(3.03)	
3 (NBu^i/Ph$_2$)	PhLi	$C_{22}H_{31}NSn$	212 (0.05)[g]	60.42	8.97	3.30	
	65	428.21	353[h] (100)	(61.71)	(7.30)	(3.27)	
3 (O/Ph$_2$)	PhLi	$C_{18}H_{22}OSn$	69	57.44	5.82		
	37	373.08	373 (3)	(57.95)	(5.94)		
3 (O/Br$_2$)	diGrignard	$C_6H_{12}Br_2OSn$	172	18.50	3.50		41.42
	9	378.67	299[j] (100)	(19.03)	(3.19)		(42.20)
4 (NBu^i/Cl$_2$)	diGrignard	$C_{10}H_{21}Cl_2NGe$	114	39.02	6.84	4.63	—
	3	298.79	299 (7)	(40.13)	(7.02)	(4.68)	(23.75)

[a] M^+.

[b] Ref. [11b]: 60%.

[c] M^+—Cl.

[d] M^+—OSiPh$_3$.

[e] M^+—Bu^i.

[f] Ph_6Si_2O. Highest fragment with tin content: SnO_2.

[g] B.p. (Torr) (°C).

[h] M^+—Ph.

[i] FD mass spectrum.

[j] M^+—Br.

Table 4. Summary of crystal data, intensity data collection (Mo radiation, ambient temperature) and refinement for **3** and **4**

	3 (NBz/Cl$_2$)	**3** (NBu^i/Cl$_2$)	**3** (O/Cl$_2$)	**3** (NBz/(OSiPh$_3$)$_2$)	**3** (NBu^i/(OSiPh$_3$)$_2$)	**3** (NMe/ClPh)	**3** (O/Br$_2$)	**4** (NBu^i/Cl$_2$)
Cryst. system, space group	Orthorhombic, *Pnma* (no. 62)	Monoclinic, $P2_1/c$ (no. 14)	Monoclinic, $C2/c$ (no. 15)	Orthorhombic, $P2_12_12_1$ (no. 19)	Monoclinic, $P2_1/c$ (no. 14)	Orthorhombic, *Pbca* (no. 61)	Monoclinic, $C2/c$ (no. 15)	Monoclinic, $P2_1/n$ (no. 14)
a, b, c (Å)	8.043(1), 9.660(1), 19.207(2)	11.347(3), 15.394(2), 7.989(1)	22.769(6), 7.104(1), 13.730(1)	13.920(2), 44.352(1), 14.169(1)	17.608(2), 13.683(2), 17.744(1)	9.185(7), 20.320(1), 15.349(4)	23.149(3), 7.161(1), 14.026(2)	11.314(2), 7.910(2), 15.272(3)
β (°)		94.72(1)	114.16(2)		96.26(7)		114.16(1)	92.92(3)
V (Å^3), Z, F(000)	1492(1), 4, 752	1390(1), 4, 656	2026(1), 8, 1120	8748(2), 8, 3552	4251(1), 4, 1712	2864(3), 8, 1448	2121(1), 8, 1408	1365(1), 4, 616
D_{calcd}, D_{exptl} (g cm^{-3})	1.687, 1.748	1.580, 1.593	1.900, 2.088	1.304, 1.302	1.289, 1.282	1.598, 1.611	2.388, 2.365	1.817, 1.806
$\sin\theta_{max}/\lambda$ (Å^{-1})	0.7035	0.7035	0.7035	0.7035	0.7035	0.7035	0.7035	0.7035
Refl.: meas., indep. (int R)	2228, 2228 (−)	5318, 3836 (0.0125)	3232, 2725 (0.0140)	10036, 10036 (−)	12593, 9828 (0.0173)	4655, 4148 (−)	4194, 3839 (0.0234)	6382, 3949 (0.044)
No. of variables (ratio refls/var)	90 (24.7)	138 (25.2)	94 (26)	823 (7.8)	463 (16.7)	149 (20)	94 (27)	129 (20.4)
R	5.14	5.59	6.15	4.87	4.48	5.73	5.45	5.99

REFERENCES

1. Part 12: Kolb, U. and Dräger, M., *Spectrochim. Acta, Part A*, 1997, **53,** 517
2. (a) Bürgi, H.-B., *Inorg. Chem.*, 1973, **12,** 2321; (b) Bürgi, H.-B., *Angew, Chem.*, 1975, **87,** 461; *Angew. Chem. Int. Ed. Engl.*, 1975, **14,** 460; (c) Dunitz, J. D., *X-Ray Analysis and the Structure of Organic Molecules*, Ch. 7, Cornell University Press, Ithaca, New York (1979); (d) *Structure Correlation*, especially chaps. 5 and 7, Eds Bürgi, H.-B. and Dunitz, J. D., VCH, Weinheim (1994); (e) For results and applications with regard to tin compounds see: Britton, D. and Dunitz, J. D., *J. Am. Chem. Soc.*, 1981, **103,** 2971.
3. (a) March, J., *Advanced Organic Chemistry, Reactions, Mechanisms, and Structure*, p. 339, 4th edn., Wiley, New York (1992): "A large amount of work has been done on this subject. Though a great deal is known, much is poorly understood, and many results are anomalous and hard to explain"; (b) For a recent monograph see: Shaik, S. S., Schlegel, H. B. and Wolfe, S., *Theoretical Aspects of Physical Organic Chemistry, The S_N2 Mechanism*, Wiley, New York (1992).
4. (a) Kolb, U., Beuter, M. and Dräger, M., *Inorg. Chem.*, 1994, **33,** 4522; (b) Kolb, U., Beuter, M., Gerner, M. and Dräger, M., *Organometallics*, 1994, **13,** 4413.
5. Musher, J. I., *Angew. Chem.*, 1969, **81,** 68; *Angew. Chem. Int. Ed. Engl.*, 1969, **8,** 54.
6. Nomenclature as used in ref. [4]: change of hybridization from $[sp^3]$ into $[sp^2(\sigma_{\mathrm{eq}})+p_{\mathrm{z}}({}^3\sigma_{ax})+n({}^3\sigma_{ax})]$, LUMO of pentacoordination $[p_{\mathrm{z}}({}^3\sigma^*{}_{ax})]$, 4-electron 3-center HOMO's $[{}^3\sigma_{ax}(n+p_{\mathrm{z}})]$.
7. The assumption of a low-lying LUMO of pentacoordination is in accord with the experimental fact that a nucleophilic attack at a pentacoordinated Si atom is faster than an attack at a tetracoordinated Si atom: Chuit, C., Corriu, R. J. P., Reye, C. and Young, J. C., *Chem. Rev.*, 1993, **93,** 1371.
8. Kolb, U., Dräger, M., Dargatz, M. and Jurkschat, K., *Organometallics*, 1995, **14,** 2827.
9. The compound **2** with R = F has an increased coordination at tin. The same holds for an analogous series of compounds with the donor C═O at tin in ref. [10].
10. Kolb, U., Dräger, M. and Jousseaume, B., *Organometallics*, 1991, **10,** 2737.
11. (a) Jurkschat, K. and Tzschach, A., *J. Organomet. Chem.*, 1984, **272,** C13; (b) Jurkschat, K., Schilling, J., Mügge, C., Tzschach, A., Meunier-Piret, J., van Meerssche, M., Gielen, M. and Willem, R., *Organometallics*, 1988, **7,** 38; (c) For the diGrignard reagents see: Blomberg, C., Schat, G., Grootveld, H. H., Vreugdendhil, A. D. and Bickelhaupt, F., *Liebigs Ann. Chem.*, 1972, **763,** 148.
12. Structural data of '**3**(O/$\mathrm{Cl_2}$)' in ref. [11b]: V/molecule 262 Å, *U*(*eq*) for 'Cl' 0.015(*ax*) and 0.033(*eq*). This work for **3**(O/$\mathrm{Cl_2}$, and O/$\mathrm{Br_2}$ in brackets): *V* 253 (265), *U*(*eq*) 0.064(*ax*) and 0.080(*eq*) [0.066(*ax*) and 0.086(*eq*)]. $\delta(^{119}\mathrm{Sn})$ and $^1J(^{119}\mathrm{Sn}-^{13}\mathrm{C})$ in ref. [11b]: 28.46 ppm and 571.0 Hz; compare with the data in Table 2. $\delta(^{13}\mathrm{C})$ in ref. [11b]: 23.25, 25.84 and 70.85 ppm. This work for **3**(O/$\mathrm{Cl_2}$, and O/$\mathrm{Br_2}$ in brackets): 21.8 (23.4), 25.5 (25.9) and 70.7 (70.8). The bromine content of '**3**(O/$\mathrm{Cl_2}$)' in ref. [11b] originates from the used ligand $\mathrm{O[(CH_2)_3Br]_2}$, as halide exchange takes place in the diGrignard reaction with $\mathrm{SnCl_4}$ [13].
13. Bräu, E., Falke, R., Ellner, A., Beuter, M., Kolb, U. and Dräger, M., *Polyhedron*, 1994, **13,** 365.
14. 6-times boat–chair conformation: **3**(NMe/$\mathrm{Cl_2}$, NMe/ClPh, NBz/$\mathrm{(OSiPh_3)_2}$, NBu^i/$\mathrm{Cl_2}$, NBu^i/$\mathrm{(OSiPh_3)_2}$) and **4**. 3-times chair–chair conformation: **3**(NBz/$\mathrm{Cl_2}$, O/$\mathrm{Cl_2}$ and O/$\mathrm{Br_2}$). Once boat–boat conformation: **3**(S/$\mathrm{Cl_2}$) [11b]. This assignment is possibly not correct; in fact, a disorder of the carbon atoms of the ring with an unresolved mixture of the boat–chair and chair–chair conformation seems to be present. In the cases of the compounds **3**(NMe/$\mathrm{Br_2}$ and NMe/$\mathrm{I_2}$) such a disorder could be resolved: Kolb, U. and Dräger, M., unpublished structure determinations.
15. Pauling bond order $\mathrm{BO} = 10^{-[1.41 \times (d-d(\mathrm{standard}))]}$ [2c,4b,16]. Single bond standard distances *d*(Sn—N/O/S/Cl/Br/C) = 2.09/2.00/2.40/2.36/2.50/2.15 Å [4b]. *d*(Ge—N) = 1.86 Å in the compound $\mathrm{Mes_3GeNH_2}$: Rivière-Baudet, M., Morère, A., Britten, J. P. and Onyszchuk, M., *J. Organomet. Chem.*, 1992, **423,** C5. *d*(Ge—Cl) = 2.14 Å according to a chemically reasonable average of distances in 12 compounds: Cambridge Crystallographic Data Base, 10/1995.
16. Pauling, L. *The Nature of the Chemical Bond, 3rd edn.*, Ch. 7, Cornell University Press, Ithaca, New York (1960).
17. (a) Harris, R. K., Kennedy, J. D. and McFarlane, W., In *NMR and the Periodic Table*, p. 309, Eds Harris, R. K. and Mann, B. E., Academic Press, London, New York, San Francisco (1978); (b) Wrackmeyer, B., *Annu. Rep. NMR Spectrosc.*, 1985, **16,** 73.
18. Smith, P. J. and Tupciauskas, A. P., *Annu. Rev. NMR Spectrosc.*, 1978, **8,** 291.
19. Pauling bond orders BO(Sn···X) of the pairs: **3**(O/$\mathrm{Br_2}$) > **3**(O/$\mathrm{Cl_2}$); **3**(NMe/ClPh) > **3**(NMe/$\mathrm{Cl_2}$); **3**(NBz/$\mathrm{Cl_2}$) > **3**(NBz/$\mathrm{(OSiPh_3)_2}$); **3**(NBu^i/$\mathrm{Cl_2}$) > **3**(NBu^i/$\mathrm{(OSiPh_3)_2}$).
20. Macharashvili, A. A., Shklover, V. E., Struchkov, Yu. T., Oleneva, G. I., Kramarova, E. P., Shipov, A. G. and Baukov, Yu. I., *J. Chem. Soc., Chem. Commun.*, 1988, 683. The ceasing of the overall *trans* influence in the central part of the series is not mentioned explicitly in the paper.
21. (a) Program CACAO (Computer Aided Composition of Atomic Orbitals): Mealli, C. and Proserpio, D. M., *J. Chem. Educ.*, 1990, **67,** 399. (b) Program HYPERCHEM: Hyperchem. Inc., 419 Philip Street, Waterloo, Ontario, Canada (1994).
22. Extended Hückel parameters $\mathrm{H_{ii}}$(eV)/exponent: C(2*s* −21.40/1.625, 2*p* −11.40/1.625); H(1*s* −13.60/1.300); Cl(3*s* −26.30/2.183, 3*p* −14.20/1.733); Ge(4*s* −16.00/2.160, 4*p* −9.00/1.850); N(2*s* −26.00/1.950, 2*p* −13.40/1.950). Compilation by: Alvarez, S., *Tables of Parameters for Extended Hückel Calculations*, Barcelona, 1985.
23. Harris, R. K., *Nuclear Magnetic Resonance Spec-*

troscopy, A Physicochemical View, Pitman Books Ltd, London (1983).

24. Discussion of heteroatom chemical shifts for the pairs of compounds Me_4M and Ph_4M ($M = {}^{29}Si$, ${}^{73}Ge$, ${}^{119}Sn$, ${}^{207}Pb$) and for the so-called sagging effect [17a] in mixed compounds $Ph_{4-n}M(p\text{-Tol})_n$ ($n = 0$–4; M = Si, Sn, Pb): Charissé, M., Mathiasch, B., Dräger, M. and Russo, U., *Polyhedron*, 1995, **14**, 2429.
25. $\delta({}^{119}Sn)$ in the series of compounds $Bu^n_2SnCl_2/Bu^n_4Sn/Bu^n_2SnPh_2$: $+122.0/-11.5/-65.9$ ppm.
26. 0° perfect tetrahedron, 90° perfect trigonal bipyramid [10].